

Metal–Metal Bonds

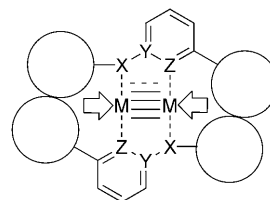
Metal–Metal Distances at the Limit: A Coordination Compound with an Ultrashort Chromium–Chromium Bond**

Awal Noor, Frank R. Wagner,* and Rhett Kempe*

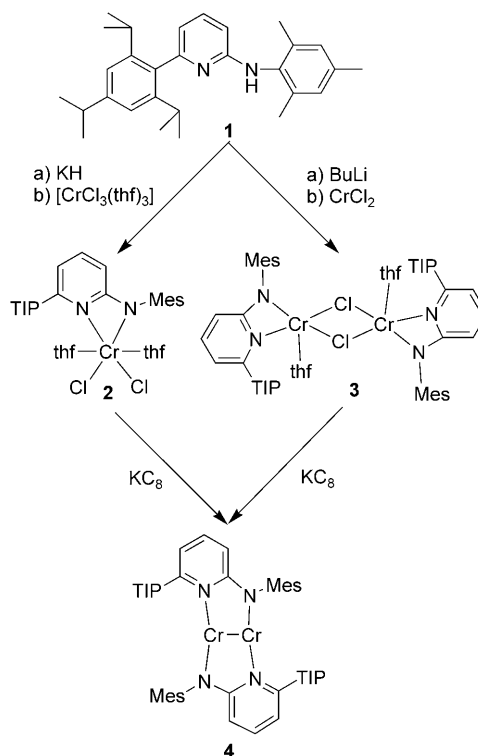
In memory of Franz Hein

The nature of the chemical bond is of fundamental importance, and has always fascinated scientists.^[1] Metal–metal bonds are of particular interest, as bond orders greater than four are known^[2,3] and are of considerable current interest.^[4] The quest for the shortest metal–metal bond is strongly linked with the element chromium^[2,5] and has very recently been reinitiated after the first observation of a bond order greater than four for this metal in a stable compound.^[3] Soon afterwards, the shortest metal–metal bond with a chromium–chromium distance of 1.80 Å was observed in a dimeric chromium complex with such a high bond order.^[6] Detailed studies on ArCrCrAr complexes (Ar = aryl) performed at the same time showed that such small values can be obtained for this class of compounds as well.^[7] Some years ago, we started working with aminopyridinato complexes of chromium^[8] and herein report the synthesis and the (electronic) structure of a bimetallic Cr^I₂ complex with a drastically shortened metal–metal distance. The very short metal–metal bond of only 1.75 Å results from a combination of Power's concept for the stabilization of bond orders higher than four,^[3,7] Hein–Cotton's principles on the realization of extremely short metal–metal bonds with bridging anionic ligands of type XYZ,^[2,9] and a minimization of additional metal–ligand interactions by optimal steric shielding (Scheme 1).

The deprotonation of **1** with potassiumhydride leads to potassium [6-(2,4,6-triisopropylphenyl)pyridin-2-yl](2,4,6-trimethylphenyl)amide, which readily reacts with [CrCl₃(thf)₃] affording complex **2** (Scheme 2). Compound **2** can be isolated as a green crystalline material in good yield. In the ¹H NMR spectrum, only broad signals can be observed, and magnetic susceptibility experiments show a magnetic moment $\mu_{\text{eff}}(300\text{ K}) = 3.2\ \mu_{\text{B}}$. When **1** is deprotonated with BuLi and allowed to react with CrCl₂ in THF, the Cr^{II} complex **3** is obtained in good yield as a green crystalline material after removal of the solvent and subsequent extraction with



Scheme 1. Shortening of the metal–metal bond by high bond order, bridging coordination of anionic ligands of type XYZ, and minimizing the additional metal–ligand interactions by steric shielding.



Scheme 2. Synthesis of **2**, **3**, and **4** (TIP = 2,4,6-triisopropylphenyl, Mes = 2,4,6-trimethylphenyl).

toluene. The molecular structure of **3** is shown in Figure 1.^[10] Compound **3** is the first Cr^{II} complex in which the deprotonated aminopyridine has a strained bidentate coordination mode and does not act as a bridging ligand.^[11] The chromium–nitrogen bond lengths clearly distinguish this compound as an amidopyridine; i.e., the anionic function of the ligand is localized on the N_{amido} atom (N2).^[12] Reduction of **4** with potassium graphite (KC₈) in THF, followed by

[*] Dr. F. R. Wagner

Max-Planck-Institut für Chemische Physik fester Stoffe

01187 Dresden (Germany)

Fax: (+49) 351-4646-3002

E-mail: Wagner@cpfs.mpg.de

A. Noor, Prof. Dr. R. Kempe

Lehrstuhl Anorganische Chemie II, Universität Bayreuth

95440 Bayreuth (Germany)

Fax: (+49) 921-55-2157

E-mail: Kempe@Uni-Bayreuth.de

[**] We thank Germund Glatz for the single crystal X-ray analyses.

Supporting information for this article is available on the WWW under <http://dx.doi.org/10.1002/anie.200801160>.

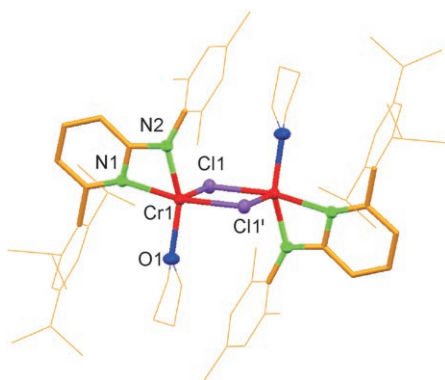


Figure 1. ORTEP of **3**. Ellipsoids for non-carbon atoms are set at 50% probability; hydrogen atoms and two toluene molecules per complex omitted for clarity. Selected bond lengths [Å] and angles [°]: N1–Cr1 2.1041(15), N2–Cr1 2.0411(14), Cl1–Cr1 2.3773(5), Cl1'–Cr1 2.6219(5), Cr1–O1 2.0869(13); N2–Cr1–N1 64.77(6), O1–Cr1–N1 98.74(5).

removal of the solvent and extraction with toluene, affords **5** as a red crystalline material in 21% yield (Scheme 2). The reduction of **3** with potassium graphite also leads to **4** (15% yield). In the ^1H NMR spectrum of the diamagnetic compound **4**, only one set of signals is observed at room temperature.

The X-ray crystal structure analysis of **4** shows it to be a bridged bimetallic complex, with an exceptionally short metal–metal distance of 1.749(2) Å (Figure 2).^[13] The hitherto



Figure 2. ORTEP of **4**. Ellipsoids for non-carbon atoms are set at 50% probability; hydrogen atoms omitted for clarity. Selected bond lengths [Å] and angles [°]: Cr1–Cr1' 1.749(2), Cr1–N2 1.998(4), Cr1–N1 2.028(4); Cr1'–Cr1–N2 98.55(13), Cr1'–Cr1–N1 96.78(13), N2–Cr1–N1 164.64(16).

shortest metal–metal bond known (1.8028(9) Å) also belongs to a bimetallic chromium complex stabilized by an N-ligand. The electronic structure of that complex was calculated, and it has an effective bond order of 4.3.^[6] For nearly 30 years an aryl chromium(II) compound, structurally characterized by Cotton and Koch^[14] and first prepared by F. Hein and Tille more than 40 years ago,^[9a] claimed to have the shortest experimentally obtained metal–metal distance of 1.830(4) Å. The chromium–chromium bond length of low-temperature laser-evaporated Cr_2 in the gas phase is about 1.68 Å.^[15]

In complex **4**, the Cr– N_{amido} bond lengths are very short (1.998(4) Å) and clearly lie below the average value for this bond (2.050 Å, dimeric chromium complexes with deprotonated aminopyridines as bridging ligands^[11]), and are shorter than the shortest reported bond of this kind (2.019 Å).^[11a] A similar situation is observed for the Cr– $\text{N}_{\text{pyridine}}$ bond lengths (2.028(4) Å for **4**, average: 2.062 Å,^[11] minimum: 2.023 Å^[11e]). These values strongly indicate a stable metal–ligand bond. A weak coordination of the amido ligand, which would then cause a maximal approach of the central atoms, cannot be an explanation for the exceptionally short metal–metal distance in **4**. However, a possible explanation could be the spatial proximity of both N-donor functions in the ligands of type XYZ (Scheme 1).

The electronic structure of **4** was studied in position space at the DFT level^[16] by means of the topological analysis of the calculated electron density and the electron localizability indicator (ELI-D),^[17] and by calculation of the delocalization index.^[18] The calculations were performed on different structural models^[19] of **4**. Below we explicitly discuss only the results for model **4'a** (structure with terminal H atoms: see Figure 3).

In analogy to the model calculations for the two already reported binuclear Cr_2 complexes with a formal quintuple bond,^[3,6] in the present case, a $(\sigma_g)^2(\pi_u)^4(\delta_g)^4$ configuration of the chromium-based MOs is also obtained. These MOs can be found in all the models within the seven highest occupied

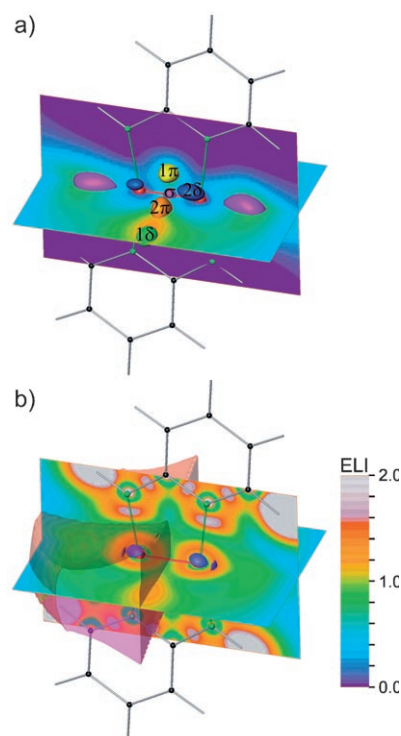


Figure 3. a) Isosurface diagram of the pELI-D contributions of $3d$ (purple), π (yellow and orange), and δ (d orbitals) (green and dark blue); The section planes show the sum of the five pELI-D contributions. b) Section plane showing (total) ELI-D; the dark blue isosurface (value: 1.44) shows the structuring of the third chromium shell; the semitransparent surface shows the QTAIM basin of one of the chromium atoms.

orbitals. The two δ_g MOs are always the HOMO and HOMO–1, and the two π_u MOs HOMO–5 and HOMO–6. Energetically, the σ_g MO and two ligand-centered MOs with a strong N_{amido} contribution can be found between these two groups. The HOMO–LUMO gap lies between 1.5 eV and 1.7 eV, depending on the corresponding model.

For further analysis, the electron density and ELI-D were calculated in position space.^[20a] As recently shown, ELI-D can be split in a physically transparent way into additive positive orbital contributions (pELI-D contributions),^[17e] where the corresponding orbital density is simply multiplied by a position-dependent weighting function (the so-called pair-volume function). An illustration of the pELI-D contributions for the five chromium-centered MOs is given in Figure 3a. The isosurfaces encompass the regions where the corresponding MOs have the highest localizability contributions (pELI-D contributions) to the total ELI-D distribution. From Figure 3a, it can be seen that the σ_g MO, the two π_u MOs, and the one δ_g MO have pELI-D maxima in the region between the two chromium atoms. The remaining δ_g MO (HOMO; 2δ in Figure 3a) has a pELI-D topology with four maxima at each atom (according to the shape of the δd orbital), and not in the interatomic region, which closely resembles a situation with two separated chromium atoms. Interestingly, this behavior is observed for only one of the two δ_g MOs. The other MO shows a strong mixing of Cr(4s) contributions, which largely eliminates the δd contributions in the direction of the ligand and reinforces those in the perpendicular direction. This results in the formation of a pELI-D maximum perpendicular to the molecular plane and relatively far from the bond axis. The sum of these five pELI-D contributions yields the pELI-D distribution shown in Figure 3a. It shows the topological points for the chromium–chromium bonding situation displayed by total (all-electron) ELI-D (Figure 3b). These are the two ELI-D maxima which are perpendicular to the molecular plane, resulting from the sum of a π_u and δ_g pELI-D orbital contribution (so-called banana bonds), and two axially situated maxima, which are not found for the less-simplified model **4a**, on the bond-opposed side of the chromium atoms. Furthermore, a significant structuring of the chromium third atomic shell signals the participation of the d orbitals in the bond formation. The electronic population of the two bonding basins in the valence region amounts to $1.8 e^-$ (banana bond) in total, and for the two bond-opposed basins only $0.3 e^-$.^[20b] The electronic population of the chromium third atomic shell, having a total of $11.8 e^-$, exceeds the value corresponding to a $3s^2p^6$ configuration by $3.8 e^-$. Therefore, the electrons for the chromium–chromium bonding interaction are not only localized in the valence region, but can also largely be found in the spatial region of the third shell of the chromium atoms, where they contribute to the above-mentioned structuring of ELI-D. The former statement can be verified by calculation of the delocalization index^[18] $\delta(A,B)$ between the third shells of both chromium atoms. A relatively high value of 2.4 for the corresponding delocalization index is found,^[21] which represents an indirect contribution in the calculation of the bond order in position space according to Ángyán, Loos, and Mayer.^[22] Thus, the bond order in the case of a symmetrical

chromium–chromium bond corresponds to the delocalization index $\delta(\Omega_{\text{Cr1}}, \Omega_{\text{Cr2}})$ between the touching density basins (QTAIM method)^[23] Ω_{Cr1} and Ω_{Cr2} of the chromium atoms. The density basin of one chromium atom is depicted in Figure 3b. It includes the complete third shell and cuts the two ELI-D bonding basins in the middle between the two chromium atoms. In the present case, a value for $\delta(\Omega_{\text{Cr1}}, \Omega_{\text{Cr2}})$ of 4.2 is found (2.4 of which results solely from the delocalization between the two chromium third atomic shells, see above), which significantly differs from the formal bond order of 5.0. However, this finding is consistent with the weakly bonding δd MO discussed above. Interestingly, a very similar bond order of 4.3 was obtained for a similar compound using natural resonance theory analysis in Hilbert space.^[6] As the δ bonds in the Cr_2 model have only a small contribution to the bond formation, and the $4s$ – $4s$ bond is energetically repulsive at the equilibrium distance,^[4b] the most important effect of these electrons for the short bond distance in Cr_2 (1.68 Å)^[15] could be the avoidance of a positive charge at the metal centers. This would then be the decisive factor which has to be overcome to realize similar short distances with formally fivefold-bonded metal atoms.

In future investigations, we are interested in minimizing the metal–metal bond through variation of the ligand environment and to explore the reactivity of the such metal–metal bonds, and to describe in detail the bonding situation for **4** in position space at an explicitly correlated level of theory.

Received: March 10, 2008

Revised: May 13, 2008

Published online: August 13, 2008

Keywords: chemical bonds · chromium · electronic structure · multiple bonds · N ligands

- [1] a) L. Pauling, *Die Natur der chemischen Bindung*, 3rd ed., VCH, Weinheim, **1973**; b) G. N. Lewis, *J. Am. Chem. Soc.* **1916**, *38*, 762–785; c) “90 Years of Chemical Bonding”: G. Frenking, S. Shaik, *J. Comput. Chem.* **2007**, *28*, 1–3.
- [2] F. A. Cotton, L. A. Murillo, R. A. Walton, *Multiple Bonds Between Metal Atoms*, 3rd ed., Springer, Berlin, **2005**.
- [3] a) T. Nguyen, A. D. Sutton, M. Brynda, J. C. Fettinger, G. J. Long, P. P. Power, *Science* **2005**, *310*, 844–847; b) M. Brynda, L. Gagliardi, P.-O. Widmark, P. P. Power, B. O. Roos, *Angew. Chem.* **2006**, *118*, 3888–3891; *Angew. Chem. Int. Ed.* **2006**, *45*, 3804–3807; c) G. Frenking, *Science* **2005**, *310*, 796–797.
- [4] a) L. Gagliardi, B. O. Roos, *Nature* **2005**, *433*, 848–851; b) B. O. Roos, A. C. Borin, L. Gagliardi, *Angew. Chem.* **2007**, *119*, 1491–1494; *Angew. Chem. Int. Ed.* **2007**, *46*, 1469–1472; c) G. Frenking, R. Tonner, *Nature* **2007**, *446*, 276–277; d) G. Merino, K. J. Donald, J. S. D’Acchioli, R. Hoffmann, *J. Am. Chem. Soc.* **2007**, *129*, 15295–15302.
- [5] U. Radius, F. Breher, *Angew. Chem.* **2006**, *118*, 3072–3077; *Angew. Chem. Int. Ed.* **2006**, *45*, 3006–3010.
- [6] K. A. Kreisel, G. P. A. Yap, O. Dmitrenko, C. R. Landis, K. H. Theopold, *J. Am. Chem. Soc.* **2007**, *129*, 14162–14163.
- [7] R. Wolf, Ch. Ni, T. Nguyen, M. Brynda, G. J. Long, A. D. Sutton, R. C. Fischer, J. C. Fettinger, M. Hellman, L. Pu, P. P. Power, *Inorg. Chem.* **2007**, *46*, 11277–11290.

- [8] A. Spannenberg, A. Tillack, P. Arndt, R. Kirmse, R. Kempe, *Polyhedron* **1998**, *17*, 845–850.
- [9] a) F. Hein, D. Tille, *Z. Anorg. Allg. Chem.* **1964**, *329*, 72–82; b) L. H. Gade, *Koordinationschemie*, Wiley-VCH, Weinheim, **1998**.
- [10] $P\bar{1}$, $a = 12.3740(7)$, $b = 12.9060(8)$, $c = 15.1170(10)$ Å; $\alpha = 71.269(5)$, $\beta = 75.700(5)$, $\gamma = 68.868(5)^\circ$ and $R_1 = 0.0375$ ($I > 2\sigma(I)$); $wR^2 = 0.0900$ (all data).
- [11] Examples of dimeric Cr^{II}_2 complexes in which deprotonated aminopyridines act as bridging ligands: a) F. A. Cotton, R. H. Niswander, J. C. Sekutowski, *Inorg. Chem.* **1978**, *17*, 3541–3545; b) J. J. H. Edema, S. Gambarotta, A. Meetsma, A. L. Spek, W. J. J. Smeets, M. Y. Chiang, *J. Chem. Soc. Dalton Trans.* **1993**, 789–797; c) F. A. Cotton, L. M. Daniels, C. A. Murillo, I. Pascual, *Inorg. Chem. Commun.* **1998**, *1*, 1–3; d) F. A. Cotton, L. M. Daniels, C. A. Murillo, I. Pascual, H.-C. Zhou, *J. Am. Chem. Soc.* **1999**, *121*, 6856–6861; e) F. A. Cotton, L. M. Daniels, P. Lei, C. A. Murillo, X. Wang, *Inorg. Chem.* **2001**, *40*, 2778–2784; f) R. Clerac, F. A. Cotton, S. P. Jeffery, C. A. Murillo, X. Wang, *Dalton Trans.* **2003**, 3022–3027.
- [12] S. Deeken, G. Motz, R. Kempe, *Z. Anorg. Allg. Chem.* **2007**, *633*, 320–325.
- [13] $P\bar{1}$, $a = 9.2100(12)$, $b = 12.2290(14)$, $c = 12.6890(15)$ Å; $\alpha = 94.314(9)$, $\beta = 105.714(10)$, $\gamma = 108.185(10)^\circ$ and $R_1 = 0.0570$ ($I > 2\sigma(I)$); $wR^2 = 0.1226$ (all data).
- [14] F. A. Cotton, S. A. Koch, *Inorg. Chem.* **1978**, *17*, 2021–2024.
- [15] V. E. Bondybey, J. H. English, *Chem. Phys. Lett.* **1983**, *94*, 443–447.
- [16] The calculations of the electronic structure were carried out at the DFT level with the program ADF: a) G. te Velde, F. M. Bickelhaupt, S. J. A. van Gisbergen, C. Fonseca Guerra, E. J. Baerends, J. G. Snijders, T. Ziegler, *J. Comput. Chem.* **2001**, *22*, 931–967; b) C. Fonseca Guerra, J. G. Snijders, G. te Velde, E. J. Baerends, *Theor. Chem. Acc.* **1998**, *99*, 391–403; c) ADF2006.01, SCM, Theoretical Chemistry, Vrije Universiteit, Amsterdam, The Netherlands, <http://www.scm.com>. The BLYP functional was used: d) A. D. Becke, *Phys. Rev. A* **1988**, *38*, 3098–3100; e) C. Lee, W. Yang, R. G. Parr, *Phys. Rev. B* **1988**, *37*, 785–789. In the case of single-point energy calculations, all electrons were explicitly included using a TZ2P basis set (triple $\zeta + 2$ sets of polarization functions) for each type of atom. The structure optimizations^[19] were performed within the frozen-core approximation (C,N: $1s^2$ core; Cr: $1s^2 2s^2 p^6$ core) using the corresponding TZP or TZ2P basis set. Calculation of the delocalization index was performed on the basis of a DFT (BLYP functional) single-point calculation with the Gaussian03 program system: f) M. J. Frisch et al. (entire citation: see Supporting Information), Gaussian 03, Revision C.02, Gaussian, Inc., Wallingford, CT, **2004**. Herein, the corresponding TZVP basis set was used: g) A. Schaefer, H. Horn, R. Ahlrichs, *J. Chem. Phys.* **1992**, *97*, 2571–2577; h) A. Schaefer, H. Horn, R. Ahlrichs, *J. Chem. Phys.* **1994**, *100*, 5829–5835.
- [17] a) The ELI-D is a scalar field which is defined in position space and momentum space. Roughly, ELI-D (γ_D^i) in position space can be regarded as a quasi-continuous weighted electronic charge distribution ρ_σ (the σ -spin electron density), where the weighting factor \tilde{V}_D (the so-called pair–volume function) is a local measure for the volume needed to build a same-spin (spin σ) electron pair:

$$\gamma_D^i(\mathbf{r}) = \rho_\sigma(\mathbf{r}) \times \tilde{V}_D(\mathbf{r})$$
 The values for ELI-D are limited to the range of positive numbers. Typically, ELI-D values up to 2.5 (except for H atoms) can be found in the chemically relevant valence region for molecules. ELI-D has been defined at explicitly correlated and at uncorrelated quantum chemical level. At the Hartree–Fock level, the ELI-D formula simplifies and strongly resembles the inverse kernel of the electron localization function (ELF) defined by Becke and Edgecombe: b) A. D. Becke, K. E. Edgecombe, *J. Chem. Phys.* **1990**, *92*, 5397–5403. Nevertheless, ELI-D should not be regarded as a generalization of the ELF. Although it is in a certain sense related to ELF, the ELI-D represents a separate quantity, which reflects one possible interpretation of the Becke ELF kernel at the correlated level of theory: c) M. Kohout, *Int. J. Quantum Chem.* **2004**, *97*, 651–658; d) M. Kohout, K. Pernal, F. R. Wagner, Yu. Grin, *Theor. Chem. Acc.* **2004**, *112*, 453–459; e) M. Kohout, F. R. Wagner, Yu. Grin, *Int. J. Quantum Chem.* **2006**, *106*, 1499–1507; f) M. Kohout, *Faraday Discuss.* **2007**, *135*, 43–54; g) F. R. Wagner, V. Bezugly, M. Kohout, Yu. Grin, *Chem. Eur. J.* **2007**, *13*, 5724–5741; h) M. Kohout, F. R. Wagner, Yu. Grin, *Theor. Chem. Acc.* **2008**, *119*, 413–420.
- [18] The delocalization index $\delta(\text{A,B})$ is a quantitative measure for the sharing of electrons between two non-overlapping regions A and B in position space: a) X. Fradera, M. A. Austen, R. F. W. Bader, *J. Phys. Chem. A* **1999**, *103*, 304–314; b) R. F. W. Bader, M. E. Stephens, *J. Am. Chem. Soc.* **1975**, *97*, 7391–7399.
- [19] Model **4a** was obtained by the exclusive relaxation of the H-atom positions based on the structural data of **4**. On the basis of **4a** in model **4b** the Cr–Cr distance was relaxed, which led to a shortening of the bond to 1.69 Å. A radical simplification of the model by substituting all substituents on the deprotonated aminopyridine with H leads to model **4'a**, for which only the newly added H-atom positions were relaxed. Therefore, the Cr, N, and C atom positions of molecule **4'a** shown in Figure 3 are identical with those for model **4a** and of the experimental structure **4**. Starting from **4'a**, the complex was completely relaxed (model **4'b**), which led to a planar molecule (C_{2h} symmetry) with a Cr–Cr distance of 1.68 Å. The consistent shortening of the Cr–Cr distance obtained by the present DFT(BLYP) calculations in complex **4b** with the original ligand and in complex **4'b** with the model ligand is caused by an incomplete treatment of the electron correlation in these calculations. It shows that the experimentally found short Cr–Cr distance is not caused by packing effects. For the coordinates of the models, see the Supporting Information.
- [20] a) M. Kohout, program DGrid, version 4.3, Dresden **2008**. b) M. Kohout, program Basin, version 4.2, Dresden, **2007**.
- [21] The delocalization index was calculated with the ToPMoD program on the basis of a single-point calculation performed with Gaussian 03:^[16f] S. Noury, X. Krokidis, F. Fuster, B. Silvi, Program ToPMoD, Université Pierre et Marie Curie, Paris, **2008**.
- [22] a) J. G. Ángyán, M. Loos, I. Mayer, *J. Phys. Chem.* **1994**, *98*, 5244–5248; b) X. Fradera, J. Poater, S. Simon, M. Duran, M. Solà, *Theor. Chem. Acc.* **2002**, *108*, 214–224.
- [23] R. F. W. Bader, *Atoms in Molecules: A Quantum Theory*, Oxford University Press, Oxford, **1994**.